Sustainable Materials and Technologies 28 (2021) e00274

Contents lists available at ScienceDirect

Sustainable Materials and Technologies

journal homepage: www.elsevier.com/locate/susmat

Acoustic and thermal characterization of a novel sustainable material incorporating recycled microplastic waste

Marco Caniato [a,*], Luca Cozzarini [b], Chiara Schmid [b], Andrea Gasparella [a]

[a] Free University of Bozen, Faculty of Science and Technology, Pizza Università 5, 39100 Bolzano, Italy
[b] Department of Engineering and Architecture, University of Trieste, Via Valerio 6A, 34127 Trieste, Italy

ARTICLE INFO

Article history:
Received 10 November 2020
Received in revised form 5 March 2021
Accepted 18 March 2021

Keywords:
Microplastics
Sustainable material
Thermal modelling
Acoustic modelling
Plastic recycling

ABSTRACT

Worldwide, high plastic consumption leads to huge waste production. Macro and microplastic litter affects habitats everywhere, but especially marine environments. Unfortunately, plastic is particularly difficult to retrieve from the sea, since it tends to break up into smaller pieces due to wind, water movement and solar irradiation. Hence, its end-of-life handling and management has become a major issue. Most of the time recovered plastic waste is landfilled or burnt, since it is composed of an assortment of different polymers and/or has been polluted by salt or other marine substances.

For these reasons, new recycling methods for marine litter, pursuing cleaner production criteria, are urgently required. This article presents a brand-new sustainable material, an eco-friendly foam made of waste microplastics incorporated into a bio-matrix. This novel open-cell material can be used as acoustic and thermal insulation for industrial, civil and maritime applications. Thus, an in-depth characterization is depicted, providing evidence of very good insulation properties and revealing how microplastics can be used to customize final acoustic and thermal performances.

1. Introduction

Generally speaking, marine litter is any object that has been produced or processed by humankind and reached the marine environment after its use. Nowadays, high plastic consumption influences our lives and this material has become the most significant type of waste in any domain, especially seawater. Worldwide, seas have been described as one of the areas most polluted by polymers, including micro- and macroplastics [5,12,54].

The amount of plastic in the sea is constantly increasing, and consequently its collection and final disposal are becoming even more important issues. Because of their small size, the microplastic particles found in water, sediment and biota can be harmful for humans [20,34]. Although many studies have shown interest in this topic, we need to do more to attain comprehensive knowledge of this problem [47,66]. In particular, we urgently require solutions for several problems concerning the handling of plastic wastes both during their life cycle and at the end of it [47,54,63]. Accordingly, plastic wastes are considered special pollutants and are therefore landfilled — a non-sustainable and often costly process. As many consumers have to pay for non-recyclable waste, a considerable amount of plastic litter finds its way to the sea. There, plastic is broken up into smaller and smaller particles, until over time they become microplastics [3,12,48,62].

Recently, rules and incentives to encourage fishermen to recover marine plastics are being discussed [53]. Once retrieved, reusing and recycling plastics is the best way to avoid landfilling and encourage differentiated waste collection, even in difficult environments [38,60,77]. Sustainable approaches like these guarantee eco-friendly products, pollutant reduction, a healthier future and better economics [33]. However, cleaner manufacturing processes are also needed to reduce the environmental impact of waste [14,15] and sustainable bio-based materials would be useful in this regard [18,71].

To this end, many studies on diverse waste recycling approaches have been published. For example, glass powder has been used as a concrete filler by Omran et al. [67], while Hasheminia et al. focused their research on diopside-based glass–ceramic foams [49]; Gong et al. [44], on the other hand, developed a foam out of recycled amber glass. Wood is also a well-studied waste product. Souza et al. show that it can be reused coupled with ink wastes [78], whereas Fongang et al. [39] proposed a cleaner production of wooden composites, and Morris analysed many recycling, landfill and burn options [61].

Likewise, plastic recycling has been the subject of many lines of research. Curlee started to discuss this topic in his book, concluding that it is associated with a positive economic balance [31]. Accordingly, El-Naga and Ragab have proposed PET waste as fillers for asphalt mixtures [36], while Al-Humeidawi and Al-Qadisiyah have discussed using

* Corresponding author.
E-mail addresses: mcaniato@unibz.it (M. Caniato), lcozzarini@units.it (L. Cozzarini), schmid@units.it (C. Schmid), andrea.gasparella@unibz.it (A. Gasparella).

https://doi.org/10.1016/j.susmat.2021.e00274

plastic in hot-mix asphalt [4]. Nevertheless, Dauvergne correctly observed that it is rather difficult to recycle plastic marine litter in such a fashion, because items are not sorted by type, are often coupled with other plastic (or non-plastic) materials and covered with marine salt [32]. Brown and Buranakarn observed that adaptive reuse systems are good approaches to follow in plastic recycling [19]; however, it is common to burn plastic wastes [35,40] or to use them as a filler for something completely different from their original use [2,26].

Natural polymers have been traditionally used in the field of regenerative medicine, thanks to their biocompatibility [73]. Among them, polysaccharides have been widely used as scaffolds, i.e., macroporous 3D bodies. Alginates, linear anionic polysaccharides (unbranched) are a common example, being available in nature. Sodium alginate is extracted from brown algae and consists of two monomeric units, β-d-mannuronate (M) bound to 1.4 and α-l-guluronate (G) [11,24,64]. Sodium alginate can be hydrolysed to form a rigid "egg-box" structure due to the selective binding of divalent cations to the G blocks of two adjacent polymer chains [45]. In fact, an interesting property of sodium alginate is its ability to ionically cross-link with bivalent cations such as Ca^{2+} [23]. It is therefore possible, using a natural low cost material, to produce trabecular structures, with very good durable properties [69,80].

Previous research [21] has shown that alginate of medium density is able to also produce foams with interesting thermal and acoustic properties. Other elements may be added to bio-matrix in order to achieve some other properties, like resilience. The use of plasticizers inside polymers is a well-known practice for increasing their flexibility. Among these, in the case of alginate foam, glycerol is already in use in similar contexts as a possible solution, being an eco-friendly plasticizer, [43,65,79]. The benefits of such novel materials in terms of environmental indices and life cycle analysis are evident [30].

The combination of sustainable foam production using alginate matrix and the insertion of plastic waste powder creates a new, cleaner, open-cell material whose potential thermal and acoustic properties may be desirable in many fields. One of these is construction. It is now known that buildings produce 40% of CO_2 emissions in the U.S. [17] and Europe [1]. Hence, thermal insulation is one of the paramount needs in the construction industry [9], while occupants demand acoustic insulation for acoustic indoor comfort [72].

We therefore set out to produce, study and characterize an innovative open-cell foam based on a bio-based polymer as matrix and microplastic litter as filler. We analysed the macro- and microscopic properties of the new material in terms of variation of filler quantity and type. A sensitivity study was performed in order to correlate physical parameters with overall performance. Finally, the thermal and acoustic properties of the material were characterized, correlating the microplastic influence to macro behaviours.

2. Materials and methods

In this research, a new bio-based eco-friendly open-cell foam is presented, and its manufacture and final thermal and acoustic properties and performance are discussed.

2.1. Foam production

Alginic acid sodium salt from brown algae (alginate, medium viscosity), Glycerol (≥99.5%), D-gluconic acid δ-lactone (GDL, ≥99.0%) and calcium carbonate ($CaCO_3$, 98%) necessary for the sol-gel process were purchased from Sigma Aldrich.

Plastics derived from industrial and domestic waste (polyethylene terephthalate bottles, foamed and expanded polystyrene) were chosen as representative of the microplastics most commonly found in the marine environment [37]. Mixed microplastic compositions were produced to test their respective influence on the properties of the resulting foam. Polyethylene terephthalate (PET) powders were obtained by grinding rigid PET foam. Flakes were obtained by grinding PET and expanded polystyrene (EPS) waste. Powder and flake size were later determined via optical microscopy.

Foam production was carried out following a sol-gel process, based on the one reported in previous works and according to a procedure pending patent devised by one of the authors [21]. Two samples were produced with the addition of glycerol as a plasticizer, according to a recipe previously reported [79]. Briefly, a three-dimensional porous hydrogel network is formed after the Ca ions crosslink with the G-blocks of the polysaccharide; these Ca ions are slowly released from $CaCO_3$, while the pH of the solution gradually decreased due to GDL hydrolysis in water. After gelation, the pores of the solid porous network are filled with water. To avoid pores collapse during water removal, freeze-drying technique was used. After gelation, the samples were frozen at −20 °C for 12 h and finally freeze-dried to remove water.The plastics derived from industrial and domestic waste (polyethylene terephthalate bottles, foamed and expanded polystyrene) were chosen as representative of the microplastics types and sizes most commonly found in the marine environment [13,37,41], i.e. polyethylene terephthalate and polystyrene with average size <500 μm. Mixed microplastic compositions were produced to test their respective influence on the properties of the resulting foam. Polyethylene terephthalate (PET) powders were obtained by grinding rigid PET foam. Flakes were obtained by grinding PET and expanded polystyrene (EPS) waste. Powder and flake size were later determined via optical microscopy. If real plastic debris collected in seawater are used, a washing procedure with deionized water to remove salts should be applied before using them in the foam production.

The compositions (g/100 ml) of the six samples tested are shown in Table 1. Samples were shaped into small cylindrical rods (diameter 80 mm, thickness 20 mm) for acoustic tests and larger, rectangular blocks (100 × 100 × 20 mm or 200 × 200 × 20 mm) for thermal characterization.

2.2. Sample size and density

Density was determined by dividing the sample mass by the sample volume. Samples were weighed on a Sartorius CP224S digital scale; volume was determined by measuring dimensions using an RS Pro digital calliper.

2.3. Morphological characterization

Plastic powders and flake sizes were assessed via optical microscopy imaging, using an Optika SZN-2 stereo microscope; statistic image analysis was performed using ImageProPlus by Media Cybernetics.

Morphological analysis of samples was performed using a Scanning Electron Microscope (SEM) Quanta250 (FEI, Oregon, U.S.A.), in high vacuum and in secondary electron mode, with 30 kV of tension and ~10 mm of working distance. Samples for SEM were obtained by cutting out small slices of approximately 10 x 10 x 2 mm (length x width x thickness) from the large samples. SEM samples were mounted on an aluminium stub with double-sided carbon tape, and gold sputtered by a Sputter Coater K550X (Emitech, Quorum Technologies Ltd., UK).

X-ray computed microtomography (X-μCT) was performed using a micro-focused X-ray source (L9181, Hamamatsu, Japan) delivering a polychromatic beam in a voltage range of 40–130 kV, with a maximum current of 300 μA and a minimum focal spot size of 5 μm. The samples for X-μCT were obtained by cutting out small cylinders of approximately 10 × 10 mm (diameter x thickness) from the large samples.

2.4. Acoustic characterization

The sound absorption coefficients of the samples were measured using an impedance tube according to the technical standard EN ISO

Table 1
Sample compositions (g/100 ml).

Sample ID	Alginate	Glycerol	$CaCO_3$	GDL	PET powder	PET flakes	EPS flakes	Total microplastics
I	1.400	–	0.150	1.125	3.500	0.500	0.125	4.125
II	2.500	–	0.150	1.125	3.500	0.500	0.125	4.125
III	1.400	–	0.150	1.125	12.500	–	–	12.500
IV	2.500	–	0.150	1.125	12.500	–	–	12.500
V	1.400	2.500	0.150	1.125	12.500	–	–	12.500
VI	1.700	2.500	0.150	1.125	6.250	0.625	–	6.875

10534-2 [52]. The data obtained for each sample were averaged over 3 exemplars with dimensions (diameter) of 45 mm (Fig. 1).

2.5. Acoustic modelling

In order to calculate the physical parameters related to the measured sound absorption, the Johnson et al. model [55] was used, taking into consideration the thermal integration proposed by Champoux and Allard [25]. Thus, an inverse identification procedure was applied to the measured values. A minimization approach (non-linear best-fit algorithm) was used in order to obtain values for five physical parameters, minimizing the difference between the test and model. The minimisation procedure is based on a bounded nonlinear best-fit scheme [57] and has been implemented in Matlab. By this procedure, the following acoustic and thermal parameters were determined:

- flow resistivity σ
- porosity (ϕ)
- tortuosity (α_∞)
- viscous characteristic length (Λ)
- thermal characteristic length (Λ').

Comparison of the measured values enabled us to focus on the foam microstructure and behaviour and to understand which parameters have the greatest influence on acoustic absorption. To this end, three different approaches were used:

(A) free inversion — a minimization approach in which all parameters are calculated without any range limitations;
(B) a second minimization approach in which a fixed porosity value, inferred from microtomography investigations, was imposed
(C) a third minimization approach in which fixed values for porosity and thermal characteristic length were both extrapolated from microtomography analyses.

The accuracy of the predicted results was computed by eq. (1), for standard deviation calculated from the experimental values, assuming that the latter represents the average value in the considered frequency range and eq. (2), where the mean difference is taken into account:

$$\sigma_{dev} = \sqrt{\frac{1}{N}\sum_{i=1}^{n}(x_i-\mu)^2} \quad (1)$$

$$\Delta_{mean} = \frac{1}{N}\sum_{i=1}^{n}|x_i-\mu| \quad (2)$$

2.6. Thermal characterization

The thermal conductivity of samples (200 × 200 × 20 mm) was measured using a Netzsch HFM 446 heat flow meter according to the technical standard ASTM C518 [10], at an average temperature of 20 °C. The heat capacity of samples (100 × 100 × 20 mm) was tested at between 15 °C and 25 °C using a Netzsch HFM 446 heat flow meter.

2.7. Thermal modelling

Porous materials can be suitable for thermal insulation of buildings and other constructions. Since they host stagnant air, they can be very useful for preventing heat dissipation and providing indoor comfort. Nevertheless, the solid matrix, i.e., the skeleton, can have a considerable influence on heat transfer throughout the material. Accordingly, it is the most transmitting element and, therefore, thorough analysis of its behaviour is of paramount importance, since it may or may not negatively affect the overall performance of the material.

2.7.1. Heat transfer in porous media

Thermal modelling is very useful for understanding how different microstructure components act and affect heat propagation within foam components. The use of a numerical approach, calibrated with measured values, then permits us to focus individually on the properties of the skeleton, the influence of the stagnant air, and any effect of the powder and plasticizer on the final thermal performance.

To this end, a porous medium is considered to be composed of a solid matrix, assumed to be non-deformable and by a grid of spaces partially occupied by fluid (stagnant air). Within this configuration, the heat exchange within the porous medium takes place through a combination of basic heat transmission mechanisms, namely conduction, convection and radiation. As far as conduction is concerned, the porous mean is modelled as a continuous medium; consequently, its properties are related to a macroscopic scale, focusing on a Volume of Interest (VOI). The VOI selected must possess the average properties of the overall medium. The VOI must also be very small compared to the size of the domain, but at the same time large enough to guarantee a significant statistical average of the microscopic properties, i.e., "representative" [16].

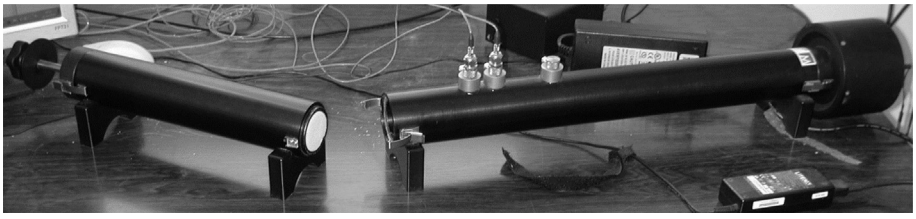

Fig. 1. Impedance tube.

The conduction of heat in isotropic media is described by the Law of Fourier (Eq. (3)):

$$q_c = -\lambda \nabla T \tag{3}$$

where λ is the thermal conductivity of the material, q_c is the heat flux caused by conduction, and ∇T is the temperature gradient.

This equation applies strictly to isotropic means. The application of Eq. (3) to heterogeneous materials, i.e., those that contain several substances with different conductive behaviours, leads to the definition of an equivalent thermal conductivity of the material [28,29,46,51,74,82].

When considering a dry material, the equivalent thermal conductivity is expressed by a general relationship (Eq. (4)):

$$\lambda_e = f(\phi, \lambda_g, \lambda_f) \tag{4}$$

where λ_e is the equivalent thermal conductivity of the material, ϕ is the porosity, λ_g is the thermal conductivity of the gas contained in the porous medium, and λ_s is the thermal conductivity of the solid part (skeleton). Since equivalent thermal conductivity also takes into account three-dimensional propagation, models are needed to perform this task. In particular, porosity, tortuosity, radiation and convection effects within pores have to be analysed.

Lastly, diffusivity and effusivity are used to evaluate the behaviour of heat over time. These parameters were assessed here using literature data and analytical approaches [76] in order to evaluate the possible difference between the diverse samples produced.

Specifically, diffusivity was computed using Eq. (5) [22]:

$$D = \frac{\lambda_e}{\rho c_p} \tag{5}$$

where λ is the overall thermal conductivity of the foam, ρ is the density and c_p is the specific heat at constant pressure.

Effusivity, on the other hand, was evaluated using Eq. (6) [8]:

$$e = \sqrt{\rho c_p \lambda_e} \tag{6}$$

2.7.2. Analytical models

Russell's model [75] and Yang and Nakayama's [85] approaches are generally used to resolve these issues. In this research, they were used to compare experimental results with the analytical ones, and thereby study the influence of the microstructure on the final macro thermal performance.

The first model is the most common in literature and it is often applied to various kinds of materials, including ceramics, packed beds, graphite and generic foams [27,58,68,81]. Indeed, it takes into account the thermal conductivity of both gaseous and solid phases, and a further parameter: porosity. This analytical approach may help to separate the influence of the fluid from that of the solid skeleton.

Yang and Nakayama focused on the tortuosity and thermal conductivity of solid and fluid phases. This model is widely used when dealing with complex foams and lattices [56,84]. It provides an analytical approach for estimating porosity on the basis of 3D cell shapes, considering tortuosity as a further parameter.

3. Results and discussion

The method described is proposed as good recycling practice. A new foam has been obtained from natural polymers and difficult-to-recycle waste. Thus, a new sustainable insulation material has been created, with beneficial properties and applications and clean production.

Table 2
Average particle size.

Waste	Analysed particles	Area [μm²]	Diameter [μm]
PET powder	132	1019 ± 1164	29.5 ± 17.8
PET flakes	57	10,518 ± 4180	110.4 ± 19.1
EPS flakes	15	1158 ± 1134	33.5 ± 16.4

3.1. Particle sizes

Table 2 reports the average sizes of the plastic powder and flakes incorporated into the foam; the size distribution is wide, but given the average size (diameter) < 500 μm, all these particles can be included in the "microplastics" category [13,41].

As can be seen from Table 2, standard deviations are very high. This means that the types of particle (powder and flakes) range widely in size, as expected. This is consistent with the process of microplastics creation, which often arises through erosion of macroplastics, grinding by sea currents and/or collisions with rocks or seabed. Another source of plastic waste is industry, which also produces items of various sizes, which may ultimately reach the seas. Lastly, urban waste may yield very different sizes of plastic litter particles.

3.2. Sample size and density

Table 3 reports foam sample sizes and densities.

It can be seen that density varies among samples. The main cause is the amount of plastic powder. However, comparing samples I and II, which feature the same quantity and composition of filler, but a different amount of alginate, it can be seen that sample II has a higher density. It can therefore be deduced that the percentage of alginate also plays a role in the determination of density, albeit to a lesser extent than microplastic powder. Furthermore, increasing the proportion of alginate provides a more compact structure with smaller pores.

3.3. Visual inspection

Some samples present stratification, with more plastic on the upper surface. Sample pictures are shown in Fig. 2. Sample I (Fig. 2 a and e) reveals unevenness in the vertical distribution of the plastic particles, with an accumulation of black EPS flakes on the upper face and light blue particles (PET flakes) on the lower side.

Sample II (Fig. 2 b and f) is more homogeneous, but with black particles (EPS flakes) on the surface and sedimentation of PET powder on the bottom. Sample III (Fig. 2 c and g) is produced with only one type of plastic (PET powder), so there is no colour stratification.

Since sample IV and V are very similar to sample III, their description is not reported for the sake of brevity. In Sample VI (Fig. 2 d and h), on the other hand, it is possible to see larger pieces of PET flakes (blue particles) on the upper surface. Powder accumulation in the lower layer is also clearly noticeable.

Table 3
Sample size and density.

ID	Diameter [mm]	Thickness [mm]	Density [kg/m³]
I	83.0	12.0	69.6
II	83.0	13.5	76.3
III	85.0	14.2	143.4
IV	84.0	14.6	143.8
V	83.5	15.0	148.8
VI	82.5	15.9	108.5

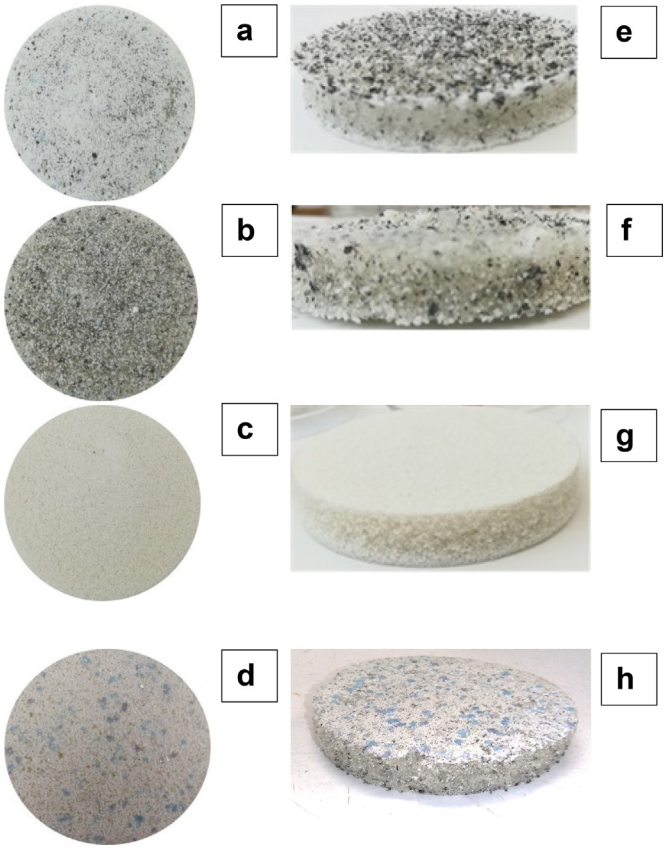

Fig. 2. Lower surface macrographs of: (a) sample I, (b) sample II, (c) sample III and (d) sample VI; section macrographs of: (e) sample I, (f) sample II, (g) sample III (h) and sample VI.

3.4. Scanning electron microscopy

Lower magnification SEM images of samples are shown in Fig. 3. Sample I (Fig. 3a) presents larger cells; sample II (Fig. 3b) has fairly regular and clean cells; sample III (Fig. 3c) features smaller cells with an irregular shape, whereas sample VI (Fig. 3d) appears to have small cells, filled with extra material.

These images confirm the influence of alginate quantity on the microstructure: sample I, presents larger cells, while sample II displays a more regular microstructure.

Higher magnification (Figs. 4–7) reveals how plastic particles are embedded between the walls of sample I cells (Fig. 4 b). In some cases, they lay on the skeleton, thereby deforming the regular shape (Fig. 4 a). Sample II rigid walls also include plastic fragments (Fig. 5 b) and in sample III the waste powder has a noticeable influence on cell morphology, with evident embedding/overlapping of plastic fragments in the cell walls (Fig. 6). Sample VI cell surfaces seem to be covered by crystals or deposits (Fig. 7 b), probably due to the presence of glycerol. However, plastic can also be seen, superficially lying on the walls rather than trapped between them (Fig. 7 a).

When comparing samples I and II, note that they were produced using the same amount of filler, but the latter contained more alginate. Sample III, on the other hand, contained the same quantity of alginate as sample I, but the largest amount of smaller-sized filler (PET powder). In the foaming process, this caused non-linear cell formation due to the influence of waste particles; these disturbed and disrupted the macro cell formation during the production process, permitting only smaller cells to develop.

3.5. X-ray computed microtomography

Table 4 shows the data resulting from X-μCT software analysis. This analysis involved about 1000 slices per sample. Sample slices at

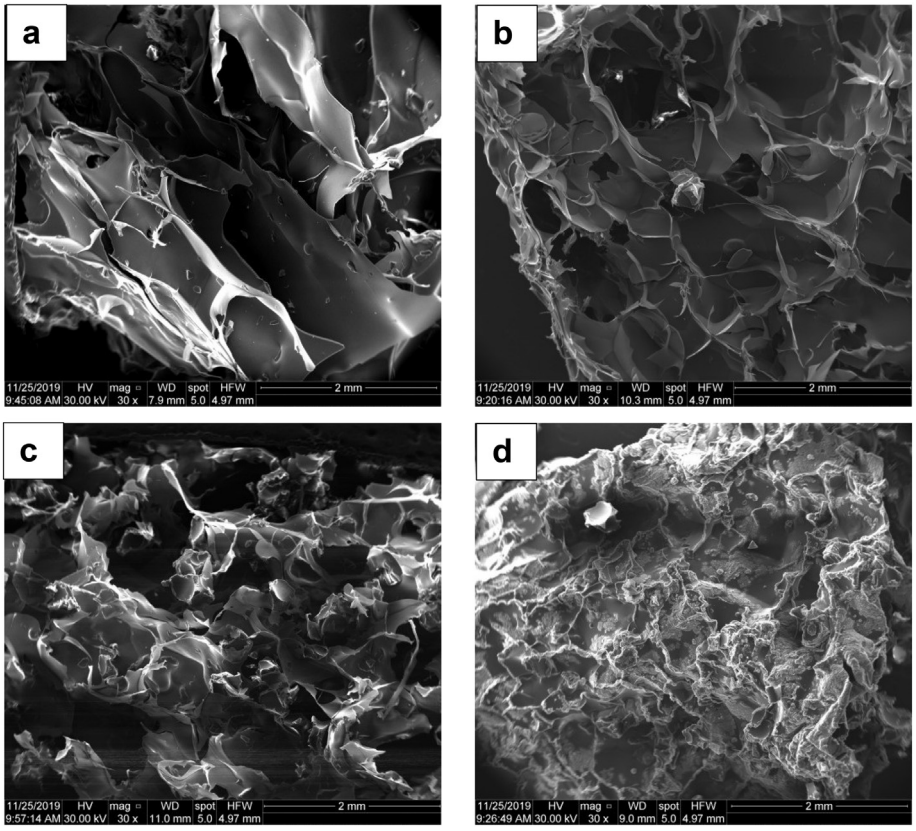

Fig. 3. Low-magnification SEM images of: (a) sample I, (b) sample II, (c) sample III and (d) sample VI.

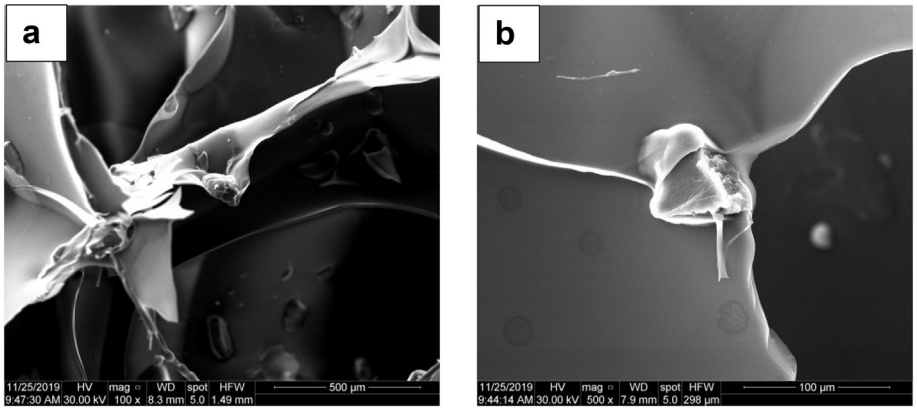

Fig. 4. High-magnification SEM images of sample I; (a) 100× and (b) 500×.

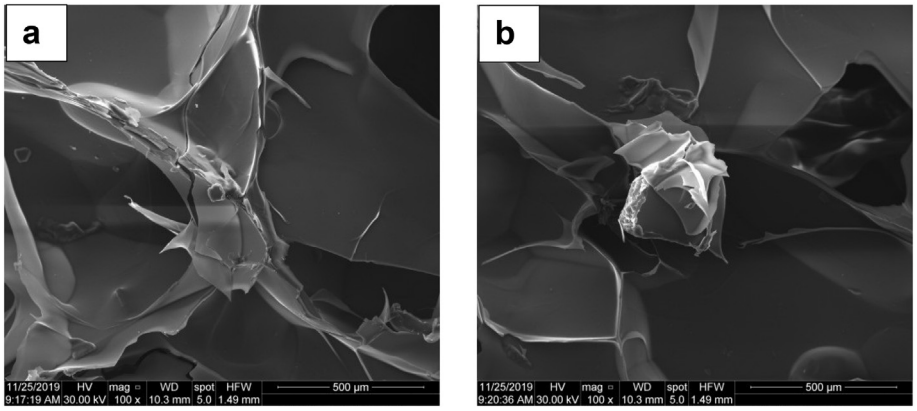

Fig. 5. High-magnification SEM images of sample II; (a) 100× and (b) 100×.

different locations along the vertical axis (z = 1, 5 and 8 mm) are shown in Figs. 8 - 11.

The lack of homogeneity in the distribution of plastic particles along the z-axis is mostly evident in samples I and II. Here the waste powder content is lower than in the others. It can therefore be seen that it is possible to differentiate powder stratification in order to produce many kinds of different materials, each with diverse performance. For instance, sample I presents surface waste accumulation, while in sample II more microplastics are present at the same z-axis. This was due to the higher percentage of alginate. In sample III, on the other hand, more particles were included, thereby improving homogeneity throughout the microstructure. In contrast, in sample VI, featuring a lower percentage of alginate, it is again possible to see the difference in powder distribution.

From the structural point of view, differences along the entire z-axis are evident; the greater amount of powder is better incorporated into the foam microstructure. This proves that a higher percentage of alginate reduces the dimensions of the pores. Conversely, glycerol does not seem significantly influence these two latter aspects.

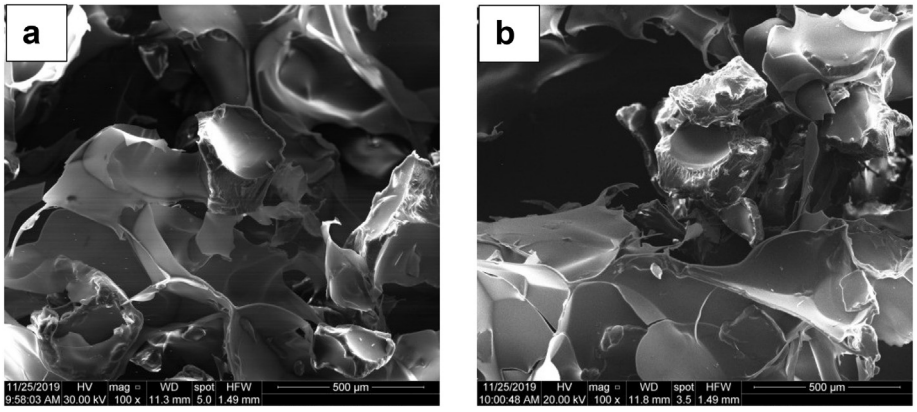

Fig. 6. High-magnification SEM images of sample III; (a) 100× and (b) 100×.

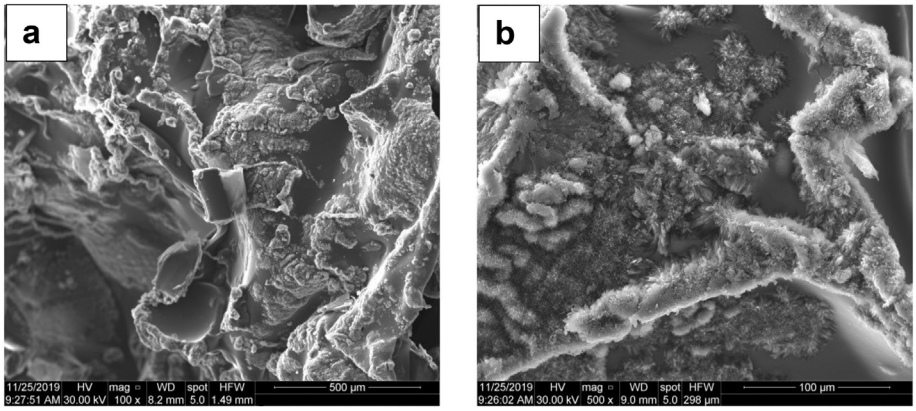

Fig. 7. High-magnification SEM images of sample VI; (a) 100× and (b) 500×.

Table 4
Statistical results from X-μCT samples.

ID	Porosity (%)	Wall thickness [μm]	Trabecular spacing [μm]	Notes
I	94.13	30.03 ± 12.65	494.96 ± 183.04	Elongated cells
II	86.66	42.97 ± 26.73	266.39 ± 110.12	Regular cell shape
III-IV-V	75.28	54.89 ± 25.97	196.85 ± 89.83	Smaller cells than samples I and II
VI	83.75	41.95 ± 18.17	248.24 ± 96.86	Medium–small cells, regular shape

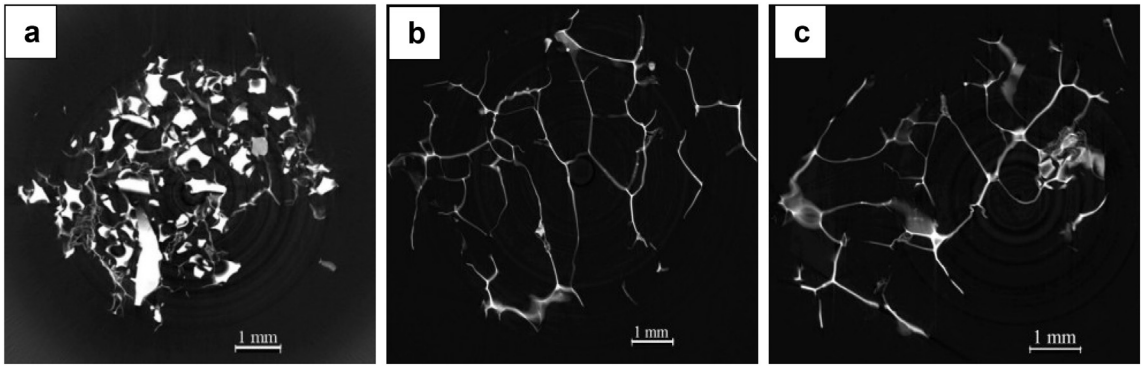

Fig. 8. X-μCT slices of sample I at Z = 1 mm (a), 5 mm (b) and 8 mm (c).

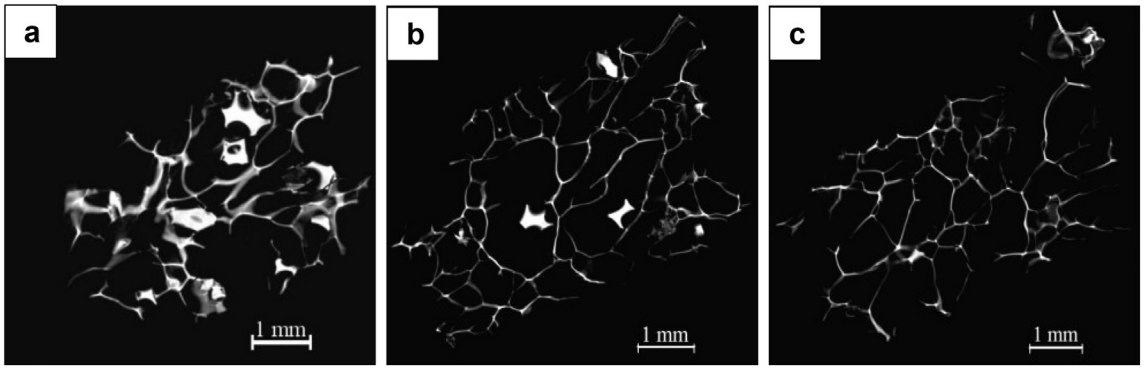

Fig. 9. X-μCT slices of sample II at Z = 1 mm (a), 5 mm (b) and 8 mm (c).

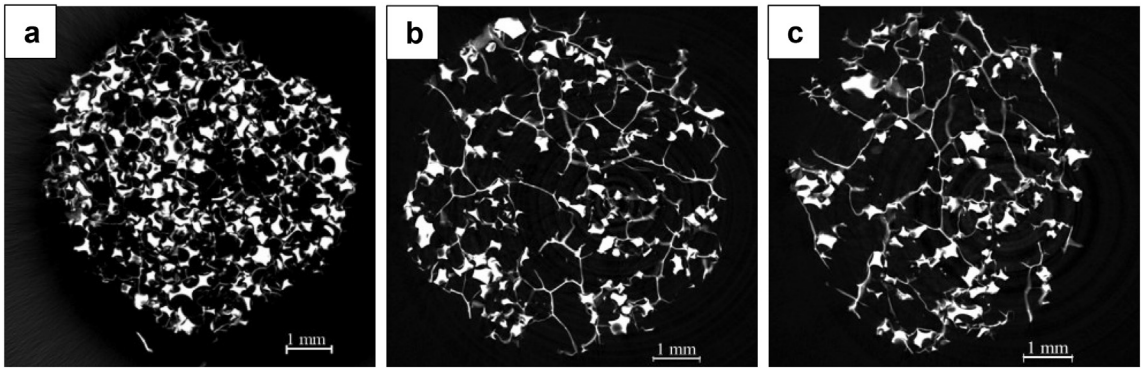

Fig. 10. X-μCT slices of sample III at Z = 1 mm (a), 5 mm (b) and 8 mm (c).

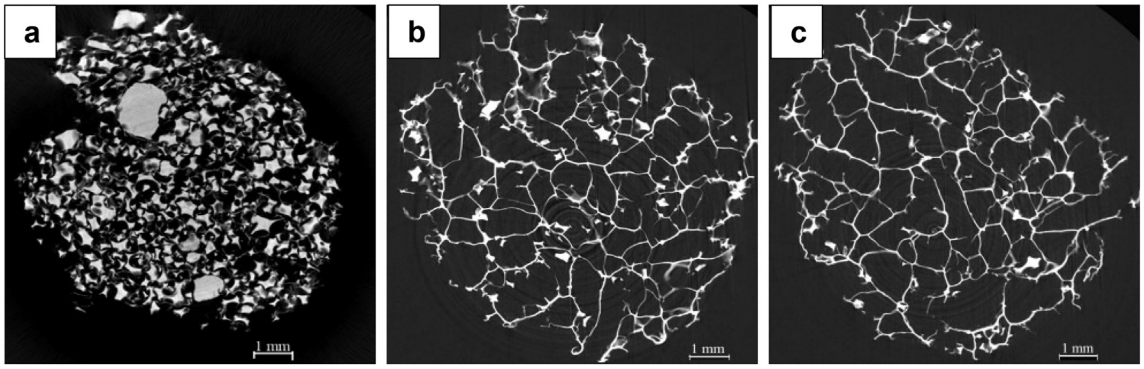

Fig. 11. X-μCT slices of sample VI at Z = 1 mm (a), 5 mm (b) and 8 mm (c).

3.6. Acoustic properties

Fig. 12 depicts a comparison of the experimental sound absorption coefficients of the six samples considered. It is interesting to note how the different foams display different macro behaviours. As can be inferred, the differences in terms of material composition can be used to provide "tailored" final acoustic performance. Sample I, for example, presents the maximum absorption at 3400 Hz, while sample II at 2600 Hz

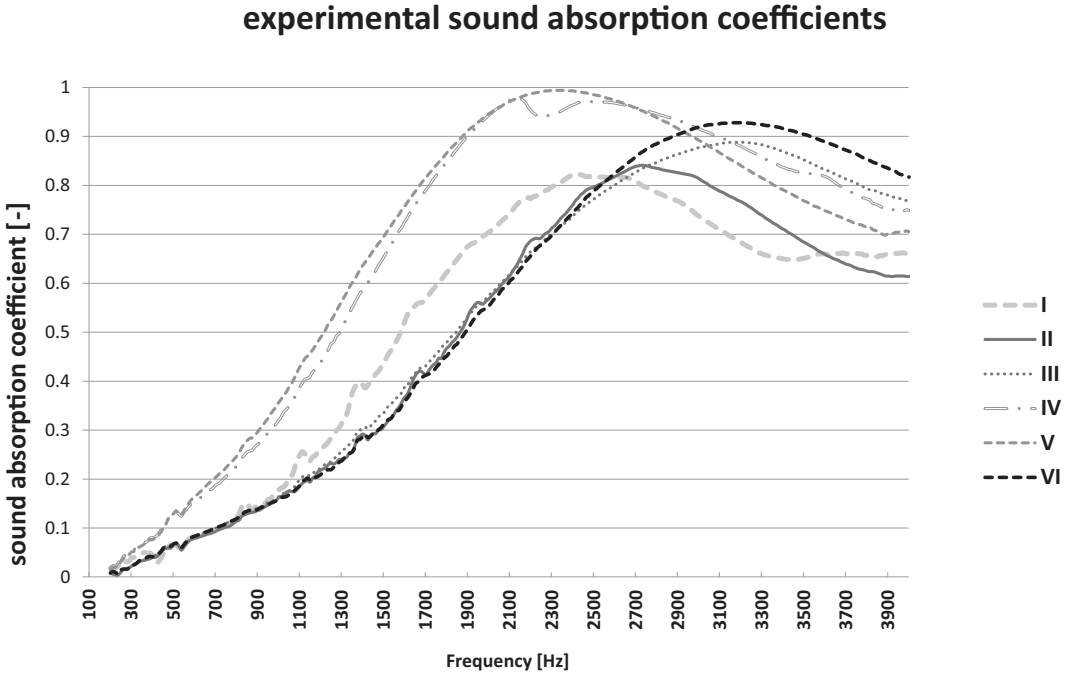

Fig. 12. Experimental sound absorption coefficients as a function of frequency.

Table 5
Results obtained from the inversion process of the tested samples, including accuracy parameters.

Sample and inversion procedure	Flow resistivity (σ) [(N s) m^{-4}]	Porosity (ϕ) [−]	Tortuosity (α_∞) [−]	Viscous characteristic length (Λ) [μm]	Thermal characteristic length (Λ') [μm]	Standard deviation (σ) [−]	Δ mean [−]
I, A	5825	0.99	5.78	119	119	0.17	0.04
I, B	6476	0.94	5.58	114	114	1.51	0.29
I, C	8494	0.94	5.71	101	350	1.32	0.25
II, A	3150	0.99	3.95	157	254	0.22	0.05
II, B	2116	0.86	4.31	252	259	0.21	0.04
II, C	1569	0.86	3.80	200	200	0.12	0.03
III, A	6287	0.98	3.15	135	136	0.24	0.05
III, B	3712	0.75	2.81	120	120	0.23	0.05
III, C	2611	0.75	3.15	137	151	0.21	0.04
IV, A	24,372	0.99	4.29	111	129	0.42	0.11
IV, B	29,266	0.75	4.45	125	125	0.41	0.09
IV, C	23,724	0.75	3.01	77	151	0.25	0.05
V, A	7288	0.99	3.59	84	118	0.06	0.01
V, B	9004	0.75	2.95	79	79	0.31	0.05
V, C	18,071	0.75	3.27	81	151	0.26	0.05
VI, A	6585	0.89	2.22	100	256	0.08	0.02
VI, B	6630	0.83	2.31	125	189	0.12	0.03
VI, C	3399	0.83	2.26	107	247	0.05	0.01

and samples III and VI at 3220 Hz. Samples IV and V focus sound absorption at 2300 Hz, also featuring good low frequency performances.

Taking into consideration that the sample thickness in this study was very small (12 mm to 14 mm), it should be possible to improve performance customization for lower frequencies by producing thicker foam layers. Note that the measured values are comparable with those of synthetic foams [70], thereby confirming that our foam represents a viable alternative.

It is evident that foams final acoustic properties are affected by the amount of microplastic powder included in the bio-matrix. One of its effects is to raise the tortuosity of the porous structure and therefore the free mean path of soundwave propagation. Another consequence is that it can vary skeleton density, mass and shape, which can be exploited to improve internal diffusion and impedance.

These facts can be confirmed using the inverse minimization process, capable of retrieving the five typical parameters related to the Johnson–Champoux–Allard model, namely air flow resistivity, porosity, tortuosity, viscous characteristic length and thermal characteristic length. Results of all numerical simulations (approaches A, B and C) are reported in Table 5.

The different compositions of the samples are evidently associated with markedly different frequency values. This highlights the resistive behaviour of the materials, which is considerably modified by different microstructures. In other words, it is evident that the microplastics included in bio-matrix skeleton influence the overall macroperformance of the foam. Another paramount role is played by the alginate quantity. Comparing sample I vs. II and III vs. IV/V, pairs with similar densities, we observe differences in both acoustic absorption peaks and overall frequency trends. In the first case, this is explained by the difference in cell morphology; for instance, sample I displays elongated cells, while sample II has a more regular microstructure (Figs. 8 and 9). In the second comparison, the difference may be attributed to the high presence of microplastic particles. This powder distribution varies from a homogeneous distribution to a concentration in the external layer, causing the absorption peaks to move to lower frequencies. More evidence of this behaviour is highlighted by the flow resistivity results. In both IV and V samples, these values rise. According to Allard and Atalla [6], this phenomenon could explain the difference in frequency trends.

Table 5 shows many other interesting results. First, it can be generally inferred that every different sample composition presents a different microstructure. Since the foremost varying element is the microplastic powder, it can be concluded that this affects the final behaviour of the foam. Another general conclusion is that the A approach (minimization approach using no limitations) does not always provide close-to-real, or even the best results. As an example, the A and B results for sample I may be misleading, even though they provide very low values of standard deviation and mean difference compared to those measured. Final acoustic behaviours clearly depend on elongated cells, but the results suggest that sample I has a homogeneous microstructure, because of the proposed equivalence between characteristic lengths. Fig. 3a and Fig. 8 clearly demonstrate that this is not true.

Furthermore, it can be ascertained that in four out of six cases, the accuracy is improved when using experimental data (II, III, IV and VI). In the other two cases, the best fit is always the minimization approach using no limitations, but still the other two approaches provide frequency trends that are acceptable, with very low standard deviation and mean difference. This indicates that it is better to use experimental data as starting values when applying inversion procedures. That being said, in this case too it is evident that waste powder affects the bio-based matrix shape, causing variations in the microstructure. Hence, it can be used to produce customized materials with different final acoustic performances, via a cleaner production chain.

3.7. Thermal characterization

Measured values of thermal conductivity λ and specific heat capacity *c* of the foam samples are reported in Table 6, as well as their diffusivity *D* and effusivity *e*. As reasonably expected, the thermal conductivity results decrease with increasing foam porosity and cell size, remaining, however, relatively consistent.

The thermal conductivity is almost in line with that of traditional materials, specifically bio-based ones [42]. The specific heat values demonstrate that the foam has a high capacity to store energy [7], while diffusivity [70] and effusivity values are similar to those of traditional insulation materials. The thermal effusivity is a measure of the property of the material to exchange heat with its surroundings. This parameter includes not only the specific heat, but also the amount of heat transfer. Therefore, the thermal effusivity is of paramount importance for describing the unsteady state

Table 6
Thermal conductivity, specific heat capacity, diffusivity and effusivity values for all tested specimens.

Sample	λ [W/m K]	*c* [J kg^{-1} K^{-1}]	D [m^2 s^{-1}]	e [W / $s^{0.5}m^2$ K]
I	0.043	1362	4.52E-07	63.34
II	0.043	1397	4.05E-07	67.86
III	0.045	1323	2.36E-07	92.19
IV	0.044	1322	2.33E-07	91.31
V	0.048	1469	2.21E-07	102.16
VI	0.043	1590	2.52E-07	86.53

Table 7
Thermal modelling results, depending on porosity.

Sample	$l_{e,R}$ [W/mK]	l_{e,Y_N} [W/mK]
I A	0.002	0.023
I B	0.014	0.04
II A	0.035	0.023
II B	0.040	0.066
III A	0.004	0.027
III B	0.066	0.010
IV A	0.004	0.027
IV B	0.066	0.010
V A	0.004	0.027
V B	0.066	0.010
VI A	0.034	0.051
VI B	0.049	0.067

heat transfer in foams [83]. As can be seen, samples III, IV and V have greater effusivity. This is because, although the specific heat capacity of samples III and IV is slightly lower than that of samples I, II and VI, their thermal conductivity is higher. In sample VI, the specific heat increases while the thermal conductivity decreases by a small amount. As a result, the effusivity is increased with respect to samples I and II.

Sample V, however, presents the greatest effusivity. Since this parameter represents the values of transmission and reflection coefficients when a thermal wave is propagating between two media (interface) [59], our evidence shows that microplastics powder enhances this phenomenon. Indeed, sample V is the one that features the highest percentage of plastic particles, as well as glycerol. Hence, it features the most complex microstructure of the samples tested (Fig. 6).

3.8. Thermal modelling

From our analysis, it was noted that the porosity and thermal conductivity of the foam skeleton had the greatest influence on the final performance values. Neither pore dimensions nor tortuosity appeared to have a significant effect on the parameters we measured; Table 7 shows the porosity variation results we obtained from the analytical models applied. The first column reports the Russell's model results, while the second column shows the Yang and Nakayama's ones. Porosity results obtained both by acoustic inversion minimizations (A) and by microtomography (B) were used in the calculations.

It can be seen that, when using the tested porosity, Russell's model tends to correctly predict the final measured values, while Yang and Nakayama's model fails, in some cases by a large margin. Although the latter model is supposed to be reliable when using a dedicated model for porosity determination, when we inserted the measured value, it did not provide reliable data.

Table 8 depicts the results for skeleton thermal conductivity variations obtained from the analytical models. As we have seen, microplastics vary the composition of the skeleton and their presence may or may not promote heat flux through foam samples. The alginate skeleton usually presents a value of thermal conductivity close to $\lambda_{s,alginate} = 0.6$ W/mK [50].

As an overall result, it can be concluded that the final macro-performance can be improved by reducing the thermal conductivity of the skeleton. It is not possible to measure the thermal conductivity of the skeleton including microplastics, but this value can be inferred through a regression approach. In this way, the thermal conductivity of the skeleton including microplastics can be estimated as $\lambda_{s,alginate+mP} = 0.3$ W/mK. It is therefore evident how the waste powder improves the overall thermal performance.

Table 8
Thermal modelling results, depending on skeleton thermal conductivity.

Sample	$l_{e,R}$ [W/mK]	l_{e,Y_N} [W/mK]	$l_{e,R}$ [W/mK]	l_{e,Y_N} [W/mK]
	$l_{s,alginate} = 0.6$ [W/mK]		$l_{s,alginate+mP} = 0.3$ [W/mK]	
I A	0.0043	0.002439	0.026	0.0233
I B	0.0250	0.014518	0.055	0.0398
II A	0.0043	0.002439	0.026	0.0233
II B	0.0603	0.03512	0.101	0.0662
III A	0.0084	0.004807	0.032	0.0266
III B	0.1135	0.066141	0.165	0.1025
IV A	0.0084	0.004807	0.032	0.0266
IV B	0.1135	0.066141	0.165	0.1025
V A	0.0084	0.004807	0.032	0.0266
V B	0.1135	0.066141	0.165	0.1025
VI A	0.0468	0.027206	0.084	0.0563
VI B	0.0743	0.043264	0.119	0.0761

4. Conclusions

This study yielded an innovative open-cell foam featuring very good acoustic and thermal properties, produced using a bio-based matrix and incorporating microplastic waste. It is thus demonstrated that a sustainable, cleaner and eco-friendly approach can be used to recycle marine waste to build a new eco-friendly material capable of acting as an acoustic and thermal insulator.

Microtomography and scanning electron microscopy investigation of the material porous microstructure highlighted its very good open-cell structure incorporating the microplastic powder. Analysis of its thermal and acoustic properties revealed that it can easily compete with traditional insulators like rock wool, polyurethane foams etc.

Furthermore, it is possible to customize the material sound absorption, adjusting it to the desired frequency range by varying the microplastic content. Indeed, we show that the waste plastic composition influences the acoustic properties, also modifying tortuosity and the thermal characteristic lengths. Inverse identification procedures were seen to provide reliable results mostly when measured porosity and thermal characteristic length values were used. This demonstrate how the Johnson- Champoux-Allard may be used to bio-based eco-friendly foams incorporating waste, only when at least two out of five parameters are known.

Moreover, thermal properties were shown to be dependent on both the porosity and thermal conductivity of the skeleton; Russell's model predicted overall thermal conductivity only when based on both measured porosity and the correct value for skeleton thermal conductivity. For this latter value, it is also demonstrated how microplastic content positively influence thermal insulation, by improving the performance of the skeleton. Moreover, the Yang and Nakayama approach failed to correctly predict final results, likely due to the fact that porosity values are imposed from the measurements.

Author contributions

M.C. designed the research and M.C., L.C. and C.S. produced the samples and carried out morphological characterization. M.C. also conducted acoustic and thermal testing, numerical simulations, acoustic inversions, thermal analyses and comparisons. C.S. and A.G. overviewed the research. M.C. wrote the paper.

Author statement

Marco Caniato: Conceptualization, Methodology, Modelling, Microstructures investigation using Xray micro-CT ans SEM, Measurements, Paper Writing, Samples production, Supervision. Luca Cozzarini: Measurements, Paper Writing, Samples production Chiara Schmid, Andrea Gasparella: Supervision.

Declaration of Competing Interest

The authors declare that they have no known competing financial interests or personal relationships that could have appeared to influence the work reported in this paper.

Acknowledgments

This study was supported by the Net4mPlastic project and co-financed by the European Regional Development Fund within in the framework of European cross-border territorial cooperation Interreg IT-HR. Specifically, this work was supported by Interreg Italy-Croatia "NET4mPLASTIC" project, CUP F76C19000000007. Furthermore, the research was performed within the framework of STAG research agreement between the Free University of Bozen and the University of Trieste.

References

[1] A.S. Ahmad, M.Y. Hassan, M.P. Abdullah, H.A. Rahman, F. Hussin, H. Abdullah, R. Saidur, A review on applications of ANN and SVM for building electrical energy consumption forecasting, Renew. Sust. Energ. Rev. 33 (2014) 102–109, https://doi.org/10.1016/j.rser.2014.01.069.
[2] G. Ahmetli, S. Kocaman, I. Ozaytekin, P. Bozkurt, Epoxy composites based on inexpensive char filler obtained from plastic waste and natural resources, Polym. Compos. 34 (2013) 500–509, https://doi.org/10.1002/pc.22452.
[3] N. Ajith, S. Arumugam, S. Parthasarathy, S. Manupoori, S. Janakiraman, Global distribution of microplastics and its impact on marine environment—a review, Environ. Sci. Pollut. Res. 27 (2020) 25970–25986, https://doi.org/10.1007/s11356-020-09015-5.
[4] B.H. Al-Humeidawi, Utilization of waste plastic and recycle concrete aggregate in production of hot mix asphalt, Al-Qadisiyah J. Eng. Sci. 7 (2014).
[5] C.G. Alimba, C. Faggio, Microplastics in the marine environment: current trends in environmental pollution and mechanisms of toxicological profile, Environ. Toxicol. Pharmacol. 68 (2019) 61–74, https://doi.org/10.1016/j.etap.2019.03.001.
[6] J. Allard, N. Atalla, Propagation of Sound in Porous Media: Modelling Sound Absorbing Materials, 2nd ed Wiley, 2009.
[7] O. Almanza, M.A. Rodríguez-Pérez, J. de Saja, Measurement of the thermal diffusivity and specific heat capacity of polyethylene foams using the transient plane source technique, Polym. Int. 53 (2004) 2038–2044, https://doi.org/10.1002/pi.1624.
[8] D.P. Almond, P.M. Patel, Photothermal Science and Techniques, Springer Netherlands, 1996.
[9] K. Amasyali, N.M. El-Gohary, A review of data-driven building energy consumption prediction studies, Renew. Sust. Energ. Rev. 81 (2018) 1192–1205, https://doi.org/10.1016/j.rser.2017.04.095.
[10] American Society for Testing and Materials International, ASTM C518-17 - Standard Test Method for Steady-State Thermal Transmission Properties by Means of the Heat Flow Meter Apparatus, 2017.
[11] T. Andersen, J.E. Melvik, O. Gåserød, E. Alsberg, B.E. Christensen, Ionically gelled alginate foams: physical properties controlled by operational and macromolecular parameters, Biomacromolecules 13 (2012) 3703–3710, https://doi.org/10.1021/bm301194f.
[12] A.L. Andrady, The plastic in microplastics: a review, Mar. Pollut. Bull. 119 (2017) 12–22, https://doi.org/10.1016/j.marpolbul.2017.01.082.
[13] C. Arthur, J. Baker, H. Bamford, Proceedings of the international research workshop on the occurrence, effects and fate of microplastic marine debris, NOAA Technical Memorandum NOS-OR&R-30. Presented at the International Research Workshop on the Occurrence, Effects and Fate of Microplastic Marine Debris, Tacoma, WA, USA, 2009.
[14] F. Asdrubali, F. D'Alessandro, S. Schiavoni, A review of unconventional sustainable building insulation materials, Sustain. Mater. Technol. 4 (2015) 1–17, https://doi.org/10.1016/j.susmat.2015.05.002.
[15] A.S.M.A. Awal, H. Mohammadhosseini, Green concrete production incorporating waste carpet fiber and palm oil fuel ash, J. Clean. Prod. 137 (2016) 157–166, https://doi.org/10.1016/j.jclepro.2016.06.162.
[16] Y. Bachmat, J. Bear, On the concept and size of a representative elementary volume (rev), in: J. Bear, M.Y. Corapcioglu (Eds.), Advances in Transport Phenomena in Porous Media, NATO ASI Series, Springer Netherlands, Dordrecht 1987, pp. 3–20, https://doi.org/10.1007/978-94-009-3625-6_1.
[17] B. Becerik-Gerber, M.K. Siddiqui, I. Brilakis, O. El-Anwar, N. El-Gohary, T. Mahfouz, G.M. Jog, S. Li, A.A. Kandil, Civil engineering grand challenges: opportunities for data sensing, information analysis, and knowledge discovery, J. Comput. Civ. Eng. 28 (2014), 04014013, https://doi.org/10.1061/(ASCE)CP.1943-5487.0000290.
[18] H. Binici, M. Eken, M. Dolaz, O. Aksogan, M. Kara, An environmentally friendly thermal insulation material from sunflower stalk, textile waste and stubble fibres, Constr. Build. Mater. 51 (2014) 24–33, https://doi.org/10.1016/j.conbuildmat.2013.10.038.
[19] M.T. Brown, V. Buranakarn, Emergy indices and ratios for sustainable material cycles and recycle options, Resour. Conserv. Recycl. 38 (2003) 1–22, https://doi.org/10.1016/S0921-3449(02)00093-9.
[20] A. Burton, White Paper - Microplastics in Aquatic Systems: An Assessment of Risk, 2020.
[21] M. Caniato, A. Travan, Method for Recycling Waste Material, 2019 EP 3216825 B1.
[22] H.S. Carslaw, J.C. Jaeger, Conduction of Heat in Solids, 2nd ed Oxford University Press, 1959.
[23] O. Catanzano, A. Soriente, A. La Gatta, M. Cammarota, G. Ricci, I. Fasolino, C. Schiraldi, L. Ambrosio, M. Malinconico, P. Laurienzo, M.G. Raucci, G. Gomez d'Ayala, Macroporous alginate foams crosslinked with strontium for bone tissue engineering, Carbohydr. Polym. 202 (2018) 72–83, https://doi.org/10.1016/j.carbpol.2018.08.086.
[24] C. Ceccaldi, R. Bushkalova, D. Cussac, B. Duployer, C. Tenailleau, P. Bourin, A. Parini, B. Sallerin, S. Girod Fullana, Elaboration and evaluation of alginate foam scaffolds for soft tissue engineering, Int. J. Pharm. 524 (2017) 433–442, https://doi.org/10.1016/j.ijpharm.2017.02.060.
[25] Y. Champoux, J. Allard, Dynamic tortuosity and bulk modulus in air-saturated porous media, J. Appl. Phys. 70 (1991) 1975–1979, https://doi.org/10.1063/1.349482.
[26] T.J. Chandni, K.B. Anand, Utilization of recycled waste as filler in foam concrete, J. Building Eng. 19 (2018) 154–160, https://doi.org/10.1016/j.jobe.2018.04.032.
[27] A. Chatterjee, R. Verma, H.P. Umashankar, S. Kasthurirengan, N.C. Shivaprakash, U. Behera, Heat conduction model based on percolation theory for thermal conductivity of composites with high volume fraction of filler in base matrix, Int. J. Therm. Sci. 136 (2019) 389–395, https://doi.org/10.1016/j.ijthermalsci.2018.09.015.
[28] X. Cheng, K. Wei, R. He, Y. Pei, D. Fang, The equivalent thermal conductivity of lattice core sandwich structure: a predictive model, Appl. Therm. Eng. 93 (2016) 236–243, https://doi.org/10.1016/j.applthermaleng.2015.10.002.
[29] Z. Chu, G. Zhou, R. Li, Enhanced fractal capillary bundle model for effective thermal conductivity of composite-porous geomaterials, Int. Communicat. Heat Mass Trans. 113 (2020) 104527, https://doi.org/10.1016/j.icheatmasstransfer.2020.104527.
[30] L. Cozzarini, L. Marsich, A. Ferluga, C. Schmid, Life cycle analysis of a novel thermal insulator obtained from recycled glass waste, Develop. Built Environ. 3 (2020) 100014, https://doi.org/10.1016/j.dibe.2020.100014.
[31] T.R. Curlee, The Economic Feasibility of Recycling: A Case Study of Plastic Wastes, 1986 (United States).
[32] P. Dauvergne, Why is the global governance of plastic failing the oceans? Glob. Environ. Chang. 51 (2018) 22–31, https://doi.org/10.1016/j.gloenvcha.2018.05.002.
[33] P.S. de Carvalho, M.D. Nora, L.C. da Rosa, Development of an acoustic absorbing material based on sunflower residue following the cleaner production techniques, J. Clean. Prod. 270 (2020) 122478, https://doi.org/10.1016/j.jclepro.2020.122478.
[34] A. Dehaut, L. Hermabessiere, G. Duflos, Current frontiers and recommendations for the study of microplastics in seafood, TrAC Trends Anal. Chem. 116 (2019) 346–359, https://doi.org/10.1016/j.trac.2018.11.011.
[35] E. Dijkgraaf, H. Vollebergh, Burn or bury? A social cost comparison of waste disposal methods, Ecol. Econ. 50 (2004) 233–247, https://doi.org/10.1016/j.ecolecon.2004.03.029.
[36] I.A. El-Naga, M. Ragab, Benefits of utilization the recycle polyethylene terephthalate waste plastic materials as a modifier to asphalt mixtures, Constr. Build. Mater. 219 (2019) 81–90, https://doi.org/10.1016/j.conbuildmat.2019.05.172.
[37] G. Erni-Cassola, V. Zadjelovic, M.I. Gibson, J.A. Christie-Oleza, Distribution of plastic polymer types in the marine environment; a meta-analysis, J. Hazard. Mater. 369 (2019) 691–698, https://doi.org/10.1016/j.jhazmat.2019.02.067.
[38] EU Commission, Energy Performance of Buildings, 2018.
[39] R.T.T. Fongang, J. Pemndje, P.N. Lemougna, U.C. Melo, C.P. Nanseu, B. Nait-Ali, E. Kamseu, C. Leonelli, Cleaner production of the lightweight insulating composites: microstructure, pore network and thermal conductivity, Ener. Build. 107 (2015) 113–122, https://doi.org/10.1016/j.enbuild.2015.08.009.
[40] H.-J. Franke, T. Shimizu, A. Nishio, H. Nishikawa, M. Inagaki, W. Ibashi, Improvement of carbon burn-up during fluidized bed incineration of plastic by using porous bed materials, Energy Fuel 13 (1999) 773–777, https://doi.org/10.1021/ef980179n.
[41] J. Gago, F. Galgani, T. Maes, R.C. Thompson, Microplastics in seawater: recommendations from the marine strategy framework directive implementation process, Front. Mar. Sci. 3 (2016)https://doi.org/10.3389/fmars.2016.00219.
[42] N.V. Gama, B. Soares, C.S.R. Freire, R. Silva, C.P. Neto, A. Barros-Timmons, A. Ferreira, Bio-based polyurethane foams toward applications beyond thermal insulation, Mater. Des. 76 (2015) 77–85, https://doi.org/10.1016/j.matdes.2015.03.032.
[43] C. Gao, E. Pollet, L. Avérous, Properties of glycerol-plasticized alginate films obtained by thermo-mechanical mixing, Food Hydrocoll. 63 (2017) 414–420, https://doi.org/10.1016/j.foodhyd.2016.09.023.
[44] Y. Gong, R. Dongol, C. Yatongchai, A.W. Wren, S.K. Sundaram, N.P. Mellott, Recycling of waste amber glass and porcine bone into fast sintered and high strength glass foams, J. Clean. Prod. 112 (2016) 4534–4539, https://doi.org/10.1016/j.jclepro.2015.09.052.
[45] G.T. Grant, E.R. Morris, D.A. Rees, P.J.C. Smith, D. Thom, Biological interactions between polysaccharides and divalent cations: the egg-box model, FEBS Lett. 32 (1973) 195–198, https://doi.org/10.1016/0014-5793(73)80770-7.
[46] G.R. Hadley, Thermal conductivity of packed metal powders, Int. J. Heat Mass Transf. 29 (1986) 909–920, https://doi.org/10.1016/0017-9310(86)90186-9.
[47] J.N. Hahladakis, Delineating and preventing plastic waste leakage in the marine and terrestrial environment, Environ. Sci. Pollut. Res. 27 (2020) 12830–12837, https://doi.org/10.1007/s11356-020-08139-y.
[48] S. Halim Hamid, Handbook of Polymer Degradation, 2nd ed CRC Press, 2020.
[49] S. Hasheminia, A. Nemati, B. Eftekhari Yekta, P. Alizadeh, Preparation and characterisation of diopside-based glass–ceramic foams, Ceram. Int. 38 (2012) 2005–2010, https://doi.org/10.1016/j.ceramint.2011.10.035.
[50] H.F. Hassan, H.S. Ramaswamy, Measurement and targeting of thermophysical properties of carrot and meat based alginate particles for thermal processing applications, J. Food Eng. 107 (2011) 117–126, https://doi.org/10.1016/j.jfoodeng.2011.05.028.
[51] C.T. Hsu, P. Cheng, K.W. Wong, Modified Zehner-Schlunder models for stagnant thermal conductivity of porous media, Int. J. Heat Mass Transf. 37 (1994) 2751–2759, https://doi.org/10.1016/0017-9310(94)90392-1.
[52] International Organization for Standardization, EN ISO 10534-2:2001 - Acoustics - Determination of Sound Absorption Coefficient and Impedance in Impedances Tubes, 2001.
[53] Italian Government, Legge Salva Mare, 2019.

[54] J.-Q. Jiang, Occurrence of microplastics and its pollution in the environment: a review, Sust. Product. Consumpt. 13 (2018) 16–23, https://doi.org/10.1016/j.spc.2017.11.003.
[55] D.L. Johnson, J. Koplik, R. Dashen, Theory of dynamic permeability and tortuosity in fluid-saturated porous media, J. Fluid Mech. 176 (1987) 379–402, https://doi.org/10.1017/S0022112087000727.
[56] N.F. Jouybari, T.S. Lundström, J.G.I. Hellström, Investigation of thermal dispersion and intra-pore turbulent heat flux in porous media, Int. J. Heat Fluid Flow 81 (2020) 108523, https://doi.org/10.1016/j.ijheatfluidflow.2019.108523.
[57] J.C. Lagarias, J.A. Reeds, M.H. Wright, P.E. Wright, Convergence properties of the Nelder–Mead simplex method in low dimensions, SIAM J. Optim. 9 (1998) 112–147.
[58] K.-Q. Li, D.-Q. Li, Y. Liu, Meso-scale investigations on the effective thermal conductivity of multi-phase materials using the finite element method, Int. J. Heat Mass Transf. 151 (2020) 119383, https://doi.org/10.1016/j.ijheatmasstransfer.2020.119383.
[59] E. Marín, Thermal physics concepts: the role of the thermal Effusivity, Phys. Teach. 44 (2006) 432–434, https://doi.org/10.1119/1.2353583.
[60] S. Meric, H. Selcuk, B. Onat, A. Ongen, Sustainable technologies for recycling and reuse: an overview, Environ. Sci. Pollut. Res. 25 (2018) 2993–2995, https://doi.org/10.1007/s11356-017-0770-z.
[61] J. Morris, Recycle, Bury, or burn wood waste biomass?: LCA answer depends on carbon accounting, emissions controls, displaced fuels, and impact costs, J. Ind. Ecol. 21 (2017) 844–856, https://doi.org/10.1111/jiec.12469.
[62] T. O'Brine, R.C. Thompson, Degradation of plastic carrier bags in the marine environment, Mar. Pollut. Bull. 60 (2010) 2279–2283, https://doi.org/10.1016/j.marpolbul.2010.08.005.
[63] S. Ogunola, P. Thava, Microplastics in the marine environment: current status, assessment methodologies, impacts and solutions, J. Pollut. Effects & Control 4 (2016) 1000161, https://doi.org/10.4172/2375-4397.1000161.
[64] G.-W. Oh, S.Y. Nam, S.-J. Heo, D.-H. Kang, W.-K. Jung, Characterization of ionic cross-linked composite foams with different blend ratios of alginate/pectin on the synergistic effects for wound dressing application, Int. J. Biol. Macromol. 156 (2020) 1565–1573, https://doi.org/10.1016/j.ijbiomac.2019.11.206.
[65] G.I. Olivas, G.V. Barbosa-Cánovas, Alginate–calcium films: water vapor permeability and mechanical properties as affected by plasticizer and relative humidity, LWT Food Sci. Technol. 41 (2008) 359–366, https://doi.org/10.1016/j.lwt.2007.02.015.
[66] M. Oliveira, M. Almeida, The why and how of micro(nano)plastic research, TrAC Trends Anal. Chem. 114 (2019) 196–201, https://doi.org/10.1016/j.trac.2019.02.023.
[67] A. Omran, A. Tagnit-Hamou, Performance of glass-powder concrete in field applications, Constr. Build. Mater. 109 (2016) 84–95, https://doi.org/10.1016/j.conbuildmat.2016.02.006.
[68] M.B. Østergaard, M. Zhang, X. Shen, R.R. Petersen, J. König, P.D. Lee, Y. Yue, B. Cai, High-speed synchrotron X-ray imaging of glass foaming and thermal conductivity simulation, Acta Mater. 189 (2020) 85–92, https://doi.org/10.1016/j.actamat.2020.02.060.
[69] D. Porrelli, A. Travan, G. Turco, E. Marsich, M. Borgogna, S. Paoletti, I. Donati, Alginate–hydroxyapatite bone scaffolds with isotropic or anisotropic pore structure: material properties and biological behavior, Macromol. Mater. Eng. 300 (2015) 989–1000, https://doi.org/10.1002/mame.201500055.
[70] A. Prociak, J. Pielichowski, T. Sterzynski, Thermal diffusivity of rigid polyurethane foams blown with different hydrocarbons, Polym. Test. 19 (2000) 705–712, https://doi.org/10.1016/S0142-9418(99)00042-2.
[71] Y.-N. Qu, J. Xu, Z.-G. Su, N. Ma, X.-Y. Zhang, X.-Q. Xi, J.-L. Yang, Lightweight and high-strength glass foams prepared by a novel green spheres hollowing technique, Ceram. Int. 42 (2016) 2370–2377, https://doi.org/10.1016/j.ceramint.2015.10.034.
[72] B. Rasmussen, Sound insulation between dwellings – requirements in building regulations in Europe, Appl. Acoust. 71 (2010) 373–385, https://doi.org/10.1016/j.apacoust.2009.08.011.
[73] M. Rinaudo, Main properties and current applications of some polysaccharides as biomaterials, Polym. Int. 57 (2008) 397–430, https://doi.org/10.1002/pi.2378.
[74] W.M. Rohsenow, J.P. Hartnett, E.N. Ganic, Handbook of Heat Transfer Fundamentals (2nd Edition), McGraw-Hill Book Co., New York, NY, 1985.
[75] H.W. Russell, Principles of heat flow in porous insulators*, J. Am. Ceram. Soc. 18 (1935) 1–5, https://doi.org/10.1111/j.1151-2916.1935.tb19340.x.
[76] A.N. Salazar, On thermal diffusivity, Eur. J. Phys. 24 (2003) 351–358, https://doi.org/10.1088/0143-0807/24/4/353.
[77] N. Singh, D. Hui, R. Singh, I.P.S. Ahuja, L. Feo, F. Fraternali, Recycling of plastic solid waste: a state of art review and future applications, Compos. Part B 115 (2017) 409–422, https://doi.org/10.1016/j.compositesb.2016.09.013.
[78] A.M. Souza, M.F. Nascimento, D.H. Almeida, D.A. Lopes Silva, T.H. Almeida, A.L. Christoforo, F.A.R. Lahr, Wood-based composite made of wood waste and epoxy based ink-waste as adhesive: a cleaner production alternative, J. Clean. Prod. 193 (2018) 549–562, https://doi.org/10.1016/j.jclepro.2018.05.087.
[79] A. Travan, F. Scognamiglio, M. Borgogna, E. Marsich, I. Donati, L. Tarusha, M. Grassi, S. Paoletti, Hyaluronan delivery by polymer demixing in polysaccharide-based hydrogels and membranes for biomedical applications, Carbohydr. Polym. 150 (2016) 408–418, https://doi.org/10.1016/j.carbpol.2016.03.088.
[80] G. Turco, E. Marsich, F. Bellomo, S. Semeraro, I. Donati, F. Brun, M. Grandolfo, A. Accardo, S. Paoletti, Alginate/hydroxyapatite biocomposite for bone ingrowth: a trabecular structure with high and isotropic connectivity, Biomacromolecules 10 (2009) 1575–1583, https://doi.org/10.1021/bm900154b.
[81] X.L. Wang, B. Li, Z.G. Qu, J.F. Zhang, Z.G. Jin, Effects of graphite microstructure evolution on the anisotropic thermal conductivity of expanded graphite/paraffin phase change materials and their thermal energy storage performance, Int. J. Heat Mass Transf. 155 (2020) 119853, https://doi.org/10.1016/j.ijheatmasstransfer.2020.119853.
[82] W. Woodside, J.H. Messmer, Thermal conductivity of porous media. I. Unconsolidated sands, J. Appl. Phys. 32 (1961) 1688–1699, https://doi.org/10.1063/1.1728419.
[83] X. Xiao, P. Zhang, Morphologies and thermal characterization of paraffin/carbon foam composite phase change material, Solar Energy Materials and Solar Cells, Dye Sensitized Solar Cells, Organic, Hybrid Solar Cells and New Concepts 117 (2013) 451–461, https://doi.org/10.1016/j.solmat.2013.06.037.
[84] C. Yang, Y. Lin, G. Debenest, A. Nakayama, T. Qiu, Lattice Boltzmann simulation of asymptotic longitudinal mass dispersion in reconstructed random porous media, AICHE J. 64 (2018) 2770–2780, https://doi.org/10.1002/aic.16088.
[85] C. Yang, A. Nakayama, A synthesis of tortuosity and dispersion in effective thermal conductivity of porous media, Int. J. Heat Mass Transf. 53 (2010) 3222–3230.